COBEM-2017-2406
DRAG REDUCTION WITH POLYMER ADDITION IN TAYLOR-COUETTE FLOW WITH TAYLOR INSTABILITIES

Ivanor Martins da Silva
Edson José Soares
Universidade Federal do Espírito Santo, Departament of Mechanical Engineering, Vitória, ES, Brazil
ivanorms@gmail.com and edson@ct.ufes.br

Renato do Nascimento Siqueira
Instituto Federal do Espírito Santo, Campus São Mateus, São Mateus, ES, Brazil
renatons.ifes@gmail.com

Rafhael Milanezi Andrade
Universidade Federal de Minas Gerais, Departament of Mechanical Engineering, Belo Horizonte, MG, Brazil
rafhaelmilanezi@gmail.com

Abstract. Drag Reduction (DR) in turbulent flow by adding small amounts of high molecular weight polymer is an important phenomenon, which has been studied for almost 70 years. This phenomenon occurs with the interaction between polymer macromolecules and turbulent vortices. However, over time, the same processes cause the breakdown of molecules, decreasing DR efficiency. Unlike the great majority of the researches in this area, which studies DR in the turbulent regime, the present work analyzes experimentally the drag reduction in the transition region between the laminar regime (absence of vortices) and the fully turbulent regime (chaotic vortices), in the space between two concentric cylinders installed in a rheometer, where the outer cylinder is fixed and the inner cylinder rotates (Taylor-Couette flow). The fluid used here is a solution of polyacrylamide (PAM) in deionized water, with the concentrations of 10, 30, 50, 100 and 400 ppm. The experiments carried out here show that the reduction of drag does not occur only in the presence of turbulent vortices (as some studies claim), but they are also perceptible in the transition region (Taylor instabilities). It is observed in the transition regime that DR increases with the polymer concentration and also with the Reynolds number, however, there is almost no degradation of the polymer in that region.

Keywords: Drag reduction, Taylor-Couette flow, Taylor instabilities.

1. INTRODUCTION

Drag Reduction (reduction in friction factor f) by addition of small amounts of polymers in fluid flows has been successfully studied for almost 70 years, since Toms (1948). This has many practical applications in engineering, since the reduction in the friction factor f also reduces the energy consumed in the pumping process. Water transport systems, suspension and sludge (Golda 1986), prevention of cavitation and reduction of turbopump noise (Sellin et al. (1982)), reduction of energy consumption in thermal systems (Gyr and Tsinober (1995)), increase in speed of ships (Larson (2003)), increase in water jet in firefighting (Fábula (1971)) are some examples of applications. Other important applications are in the biomedical area, such as the elimination of atherosclerosis (Mostardi et al. (1978) and Unthank et al. (1992)) and prevention of death by hemorrhagic shock, according to Kameneva et al. (2003).

The phenomenon of drag reduction is extensively studied in ducts, since this configuration reflects better the practical applications, as well as in channels. However, equally important for understanding the phenomenon, but at a reduced cost are studies on rotational geometries (concentric cylinders, plates and discs). Almost all of the research is in turbulent flows. The literature in general mentions that drag reduction occurs due to the interaction between the polymer molecules and the turbulent flow vortices. Such interaction is responsible for drag reduction, however, it also causes the macromolecules to break down, which reduces the efficiency of the polymer. The understanding of this process becomes the key point for the development of more efficient polymers and also for a better theoretical understanding of the fundamentals of the reduction of drag. On the other hand, the understanding of this phenomenon is difficult due to the lack of a universal description of the turbulence and the complexity of the constitutive equations used to describe the rheology of polymer solutions (Crumeyrolle e Mutabazi (2002)). Arias and Peixinho (2017) conducted a study on the

torque variation in a Taylor-Couette flow with polymer solution, with the inner cylinder rotating and the fixed external cylinder. They found that the torque in the inner cylinder is modified compared to a Newtonian fluid with the same viscosity, revealing different flow patterns. For large concentrations of polymers, they observed six different types of isolated vortex pairs, depending on the rate of deceleration.

The objective of the present work is to study of drag reduction by addition of polymer in water, in a rotating of concentric cylinders, called here rotor (inner cylinder - in movement) and cup (external cylinder - static). The flow in this geometry is referred to in the literature as Taylor-Couette flow. The study focuses on the transition regime between laminar flow (absence of vortices) and fully turbulent flow (presence of chaotic vortices). This transition flow is characterized by the presence of vortex pairs, called Taylor vortices, responsible for generating a complex but still laminar flow. These vortices are cylindrical, have a diameter approximately equal to the distance between the rotor and cup walls and arise when the Taylor number exceeds the critical value of $Ta = 1700$ (Pereira and Soares (2012)). The Taylor number is defined according to Eq. 6. The first studies on instabilities in Taylor-Couette configuration with polymer solutions were published by Ginn and Denn (1969). By increasing the speed of the rotor, the vortices become less cylindrical, passing to a wavy form of greater instability. It is also observed the formation of small secondary vortices, known as Gortler vortices (Lee et al (1995)). With increasing rotation the flow becomes extremely complex and totally chaotic. The Taylor vortexes occur in a range of $Ta = 1700$ to 160000. Pereira and Soares (2012) divide the flow into Taylor-Couette geometry and three regions: The 1st region ($0 < Ta < 1700$), where the flow is viscometric, with the absence of vortices ($Re < 200$). The 2nd region ($1700 < Ta < 160000$), where the flow is laminar with Taylor instabilities. The 3rd region ($Ta > 160000$), where turbulence is fully developed. They conclude that the drag reduction is only clear in the 3rd region.

2. EXPERIMENTAL APPARATUS AND PROCEDURE

In this work, the experiments of drag reduction are done on the Taylor-Couette geometry, which is formed by two concentric cylinders, in which the outer cylinder is fixed to the base of a rheometer and the inner cylinder, attached to the rotor of the equipment, rotates with known rotation and torque. The tests are carried out on a commercial rheometer, model HAAKE MARS II, manufactured by the German company Thermo Scientific. In the Taylor-Couette geometry used, the radii are $R_i = 20.71$ mm and $R_o = 21.70$ mm, the height of the rotor is $L = 55$ mm and the gap is $b = 3,0$ mm. R_i is the radius of the inner cylinder (rotor) and R_o is the radius of outer cylinder (cup).
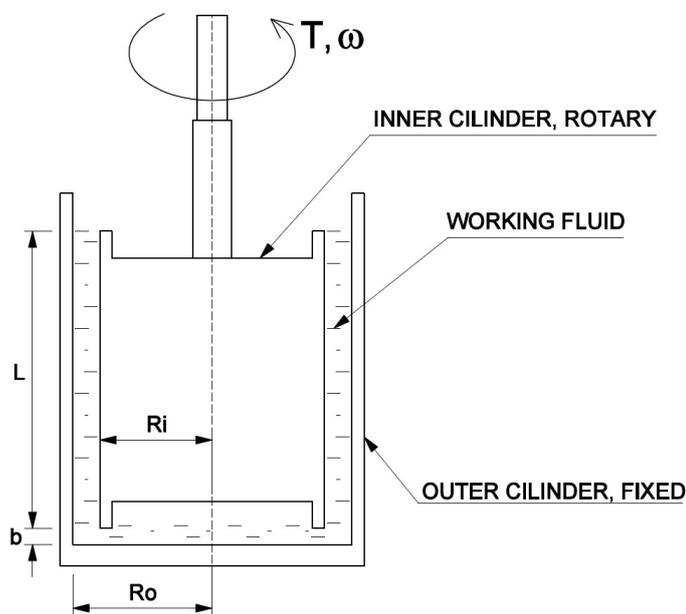

Figure 1. Schematic drawing of the Taylor-Couette experiment (out of scale).

The rheometer measures only the torque T (N.m) and the angular velocity of the motor that drives the rotor n (rpm), all quantities of interest in the experiment with the Taylor-Couette geometry are calculated from these two measurements. The shear rate ($\dot{\gamma}$) is determined as a function of the angular velocity n by Eq. (1),

$$\dot{\gamma} = K\omega = K\left(\frac{2\pi n}{60}\right) \tag{1}$$

Where K is the geometric factor, calculated by Eq. (2) as a function of the internal radii R_i and the external radius R_o of the geometry.

$$K = \frac{2R_o^{\,2}}{R_o^{\,2} - R_i^{\,2}}$$ (2)

The shear stress τ is determined as a function of the torque T, as shown in Eq. (3), while the Fanning friction factor f, based on the characteristics of the radius of the rotor R_i and the speed of the rotor surface u, is given by Eq. (4).

$$\tau = \frac{T}{2\pi R_i^{\,2} L}$$ (3)

$$f = \frac{2\tau}{\rho u^2} = \frac{2\tau}{\rho(\omega R_i)^2}$$ (4)

The Reynolds Re number of the flow is also defined as a function of the speed of the rotor u and the radius of the rotor, according to Eq. (5).

$$\mathrm{Re} = \frac{\rho h u}{\eta} = \frac{\rho h(\omega R_i)}{\eta}$$ (5)

Where η is the viscosity of the polymer solution, $u = \omega R_i$ is the characteristic speed and $h = R_o - R_i$ is the gap of this geometry. In order to better evaluate the region of transition between the laminar and turbulent regimes in Taylor-Couette geometry, we use the Taylor number (Ta), given by Eq. (6).

$$Ta = \frac{R_i h^3 \omega^2}{\nu^2}$$ (6)

Where ν is the kinematic viscosity.

In the present work five polyacrylamide solutions (PAM) of molecular weight $M_v = 5.0 \times 10^6$ g/mol were tested at the concentrations of 10, 30, 50, 100 and 400 ppm, each with Reynolds numbers of 300, 600 , 920, and 2180. Polyacrylamide was purchased from Sigma-Aldrich. In preparing the solutions, the powdered polymer was slowly deposited on the surface of the solvent (deionized water). First, a stock solution of 400 ppm was prepared and, from this, the less concentrated solutions of 10, 30, 50 and 100 ppm were diluted. This procedure facilitates the weighing of the polymer, avoiding greater inaccuracies in the weighing of quantities too small. After the preparation of the 400 ppm solution, 96 hours were waited, in which a test was performed evaluating the viscosity of the sample, accelerating the rotor from 0 to 3000 rpm in 600 seconds, with acquisition of 600 points of linear form. This test was repeated with a sample of the 400 ppm solution within 120 hours and 144 hours after the preparation thereof. By comparing the results of the three tests and checking their repeatability, it was found that the polymer solution was completely dissolved. From this stock solution of 400 ppm, the less concentrated solutions of 10, 30, 50 and 100 ppm were produced with the addition of deionized water. A further 24 hours were waited for these solutions to completely dissolve. To avoid any degradation before the start of the experiments, no stirrer or mixer was used. The 3000 rpm limit was used on the rheometer because from that rotation the flow becomes very unstable. The viscosity tests were done on double-gap geometry, due to the larger contact area and consequently greater precision in the measurement. Fig. 2 shows the viscosity as a function of the rotational speed of the rotor for the stock solution of 400 ppm, analyzed with 96, 120 and 144 hours.

Pereira and Soares (2012) tested the diffusion of a solution of 100 ppm of polyacrylamide in deionized water and found that with 24 hours the solution is already dissolved, presenting tests with 24, 48 and 96 hours after preparation of the solution. However, as the stock solution prepared in the present work is 400 ppm, we expect a longer diffusion time, because the higher the concentration. No tests were performed to verify the lowest diffusion time of the solution.
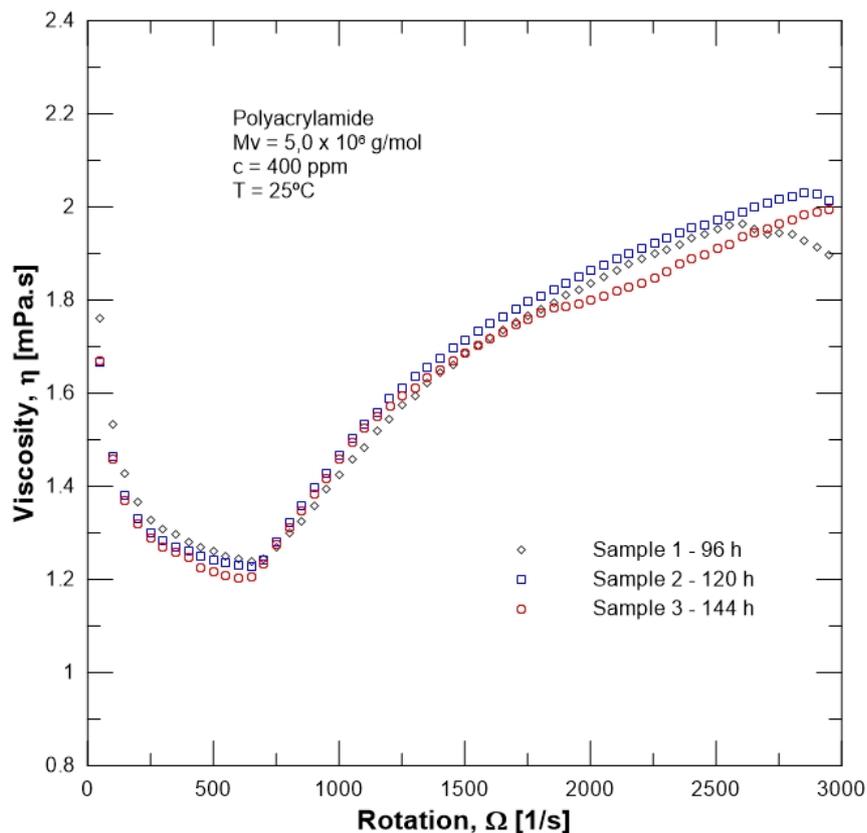
Figure 2. Natural diffusion time of the polyacrylamide in deionized water.

The rheometer used here is assisted by a computer and is equipped with a thermostatic bath capable of providing precise temperature control. All the experiments were carried out at a temperature of 25ºC.

3. RESULTS AND DISCUSSION

Firstly, experiments were carried out to detect in which Reynolds number the laminar flow ends, for which tests were made with several Newtonian fluids, in order to show the Fanning friction factor for a wide Reynolds number range, as shown in Fig. 3. The tests were carried out with soy oil, deionized water with 10% polyethylene glycol (PEG), deionized water with 50% corn glucose and pure deionized water. The graph shows, a theoretical curve fit with $f = C/Re$, where $C = 2.5$ is the constant chosen to fit this curve. It is also observed in this graph that the critical Reynolds is $Re_c = 200$, where the laminar flow (vortex augmentation) ends, seen in the graph where the points associated to the experimental results depart from the theoretical curve $f = C/Re$.

In the transition and turbulent regimes there is a better agreement in the measured friction factor for the different fluids when compared to the laminar regime. This occurs because the shear stresses are very low in the laminar region and decreasing measurement accuracy. These experiments were carried out with the rotor kept in constant rotation for three minutes at each rotation, starting from 10 up to 3000 rpm.

Another type of analysis is presented in Fig. 4, to verify where the drag reduction starts, characterized by the decrease of the friction factor f. These experiments were performed with the rotor accelerating from 0 to 1250 rpm, over a period of 30 minutes in the Taylor-Couette geometry, with the solutions of 10, 30, 50, 100 and 400 ppm of polycylamide (PAM) dissolved in deionized water. The results are compared with two Newtonian fluids, deionized water solutions with 10% polyethylene glycol (PEG) and 50% corn glucose. It can be observed that for a $Re = 400$, the PAM curves begin to move away from the Newtonian fluid curves, characterized by a reduction in the friction factor. From this point onwards, as the Reynolds number increases, the curves for each concentration also begin to differentiate, and this difference becomes more noticeable as Re increases. From 100 ppm, the friction factor no longer decreases with concentration.
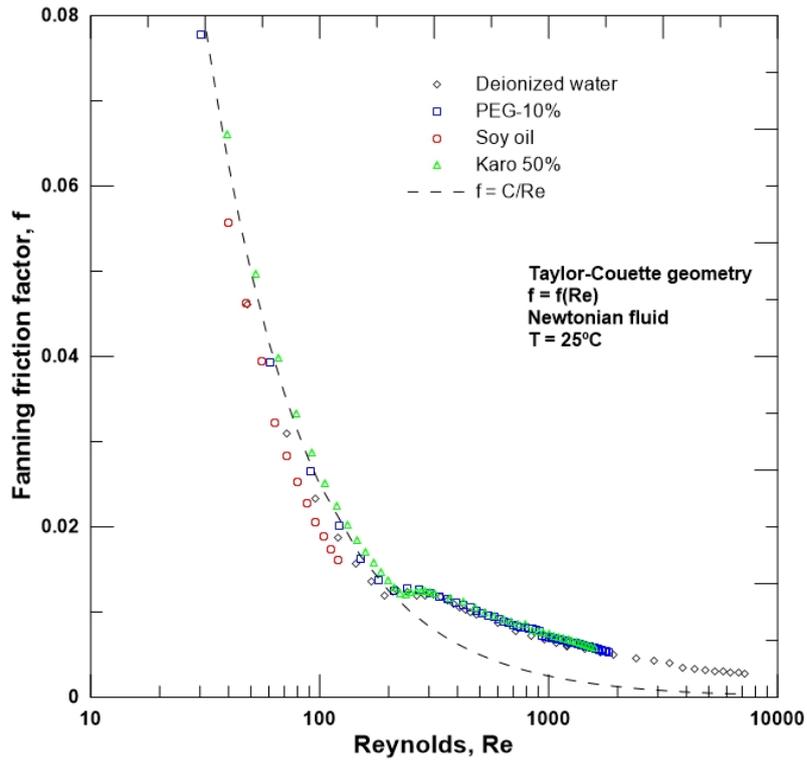
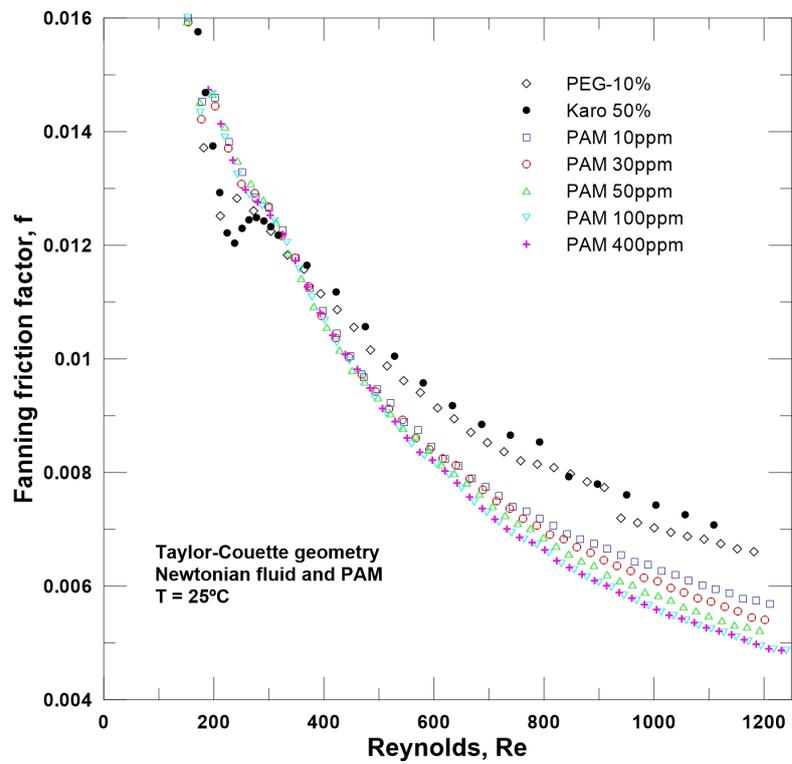Figure 3. Fanning friction factor as a function of Reynolds, for Newtonian fluids, in Taylor-Couette geometry.

Figure 4. Fanning factor friction as a function of Reynolds and drag reduction start point.

3.1 Drag reduction in the transition regime, compared to turbulent regime

The experiments shown in Fig. 5 are made by printing a constant rotation to the rotor and evaluating the drag reduction as a function of time. In this study it is also evaluated how the drag reduction varies with the concentration and the Reynolds number. Firstly, there is a reduction of drag in the 2nd region (1700 <Ta <160000), unlike that proposed by Pereira and Soares (2012), ie, DR occurs not only in the presence of chaotic vortices but also occurs where there are vortices from Taylor. It is observed that the drag reduction in the transition regime is smaller than that of the turbulent regime, but still has significant values. In addition to the drag reduction, it is also noticed that *DR* increases with the concentration and the number of Reynolds, similar to what happens in the turbulent region. Figure 5 shows three graphs in the Taylor instability region, with *Re* = 300, 600, 920 and *Ta* = 4300, 17200, 40600, respectively, and a graph for the turbulent region (*Re* = 2180 and *Ta* = 228000). In Fig. 5A, there is practically no drag reduction, the curves are close to zero and there is no clear separation between the results of each concentration. The solution with a concentration of 30 ppm seems to stand out from the others. However, from 500 seconds, there is no distinction between curves. For this Reynolds number the PAM solutions present average *DR* values around 2%, which can be considered negligible.
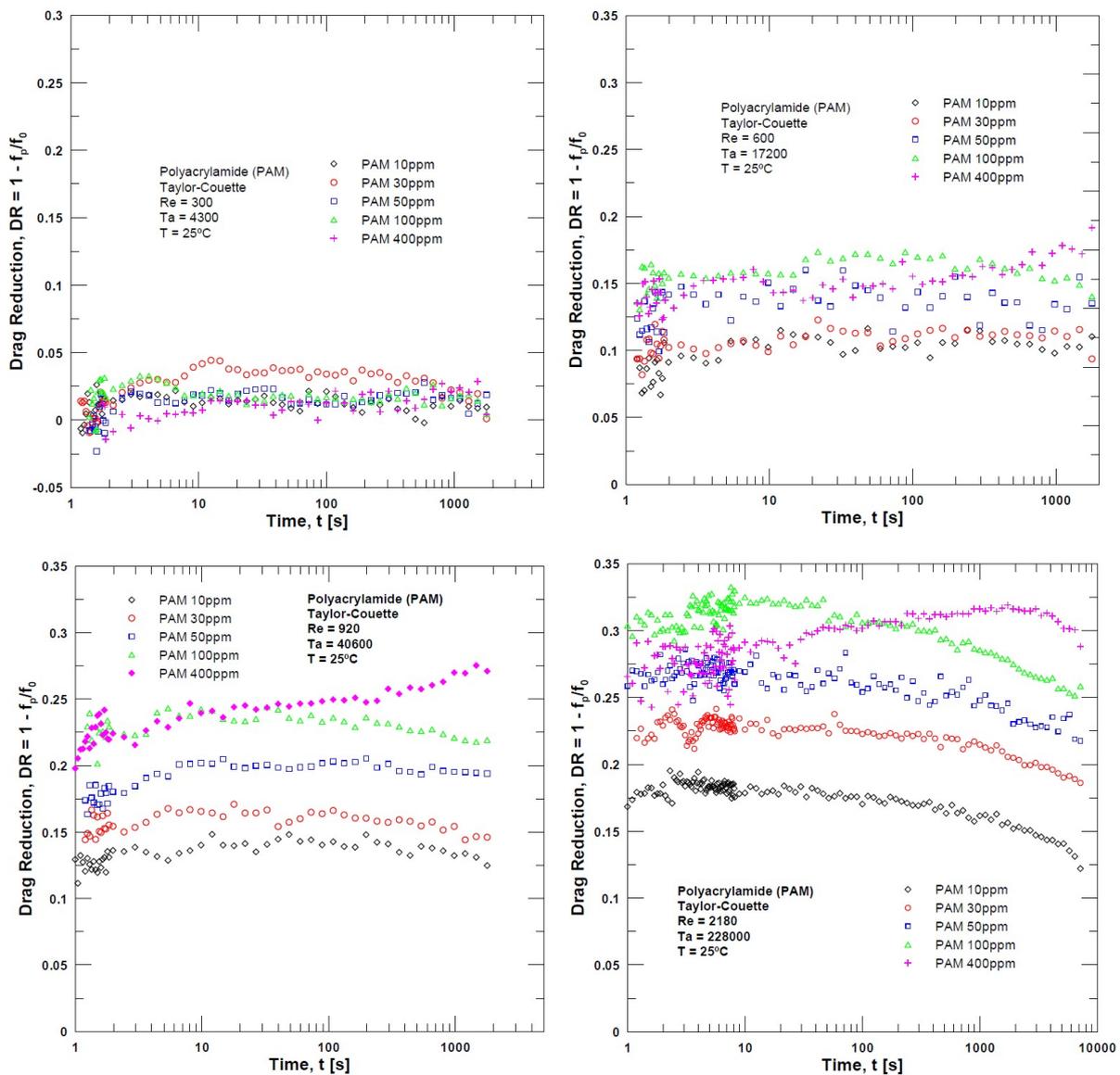

Figure 5. Drag reduction versus time for *Re* = 300, 600, 900 e 2180.

In Fig. 5B, we can clearly state that there is drag reduction, and that it increases with the polymer concentration. The average *DR* results are: 10.28% (10 ppm), 10.95% (30 ppm), 13.08% (50 ppm), 16.13% (100 ppm) and 15.24% (400 ppm). For *Re* = 920 (Fig. 5C), even in the region of the Taylor instabilities (*Ta* = 40600), the drag reduction is greater

and the results of each concentration are more clearly dissociated, mean *DR* is 13.8% (10 ppm), 15.9% (30 ppm), 19.6% (50 ppm), 23.2% (100 ppm) and 24.5% (400 ppm). It is also noted that *DR* does not vary over time for concentrations of 10 to 100 ppm, but for the concentration of 400 ppm the drag reduction equals to that of *c* = 100 ppm to about 100 seconds, then increases slightly, from 25% to 27.5%. Experimental studies in the literature (Pereira and Soares (2012), Pereira et al (2013)) show that for a constant Reynolds, the turbulent drag reduction increases at the beginning, reaches a maximum value, then there is a fall, due to polymer degradation, until asymptotic at a constant value over time. Thereafter, the breaking of the molecules is interrupted and a lower molecular weight is reached, as observed by Choi et al. (2000), Nakken et al (2001), and Vanapalli et al (2005). These authors also show that the higher the polymer concentration the longer the time taken to reach the maximum drag reduction (DR_{max}) because, at the beginning, energy is removed from the flow to stretch the macromolecules and polymer molecules in the more concentrated solutions, consequently, a greater amount of energy is spent in this process of stretching. This explains why, until *t* = 100 s, the 400 ppm solution has the same *DR* as the 100 ppm solution, after which time the more concentrated solution will have a higher *DR*, reaching 27.5% versus 22.5% of the least concentrated solution in *t* = 1800 s.

A series of experiments were also done in the fully turbulent regime, with *Re* = 2180 and *Ta* = 228000, as shown in Fig. 5D, where Taylor vortices cease to exist to give rise to completely chaotic vortices (*Ta* > 160000). The time of this experiment was higher (7200 s) than those in the region of the Taylor instabilities (1800 s), in order to better evaluate the polymer degradation, which is more sensitive in this flow regime. Differently from the other Reylolds numbers, for *Re* = 2180 a decrease of *DR* with time for all the solutions is noticed, due to polymer degradation. The 400 ppm solution only reaches DR_{max} at *t* = 2000 s, while the 100 ppm solution reaches this point with only 10 seconds. Another characteristic of the flow with Taylor instabilities (transition region) is that the shear stresses vary (oscillate) more than in the turbulent region, so the points of these experiments tend to get much more scattered across the graph. In the figures of this work a filter was applied to reduce this effect.

3.2 Polymer degradation in the region of Taylor instabilities

In the literature many works are dedicated to the experimental analysis of the polymer degradation in turbulent flows in different geometries, such as ducts, channels, flat plates, cylinders and rotary disks. It is known that molecular divisions are heavily influenced by the physicochemical characteristics of the polymers, solvent quality, concentration, molecular weight, temperature and turbulent intensity. However, such effects are not yet sufficiently exploited and their effects on the mechanism of degradation require studies (Pereira and Soares (2012)).
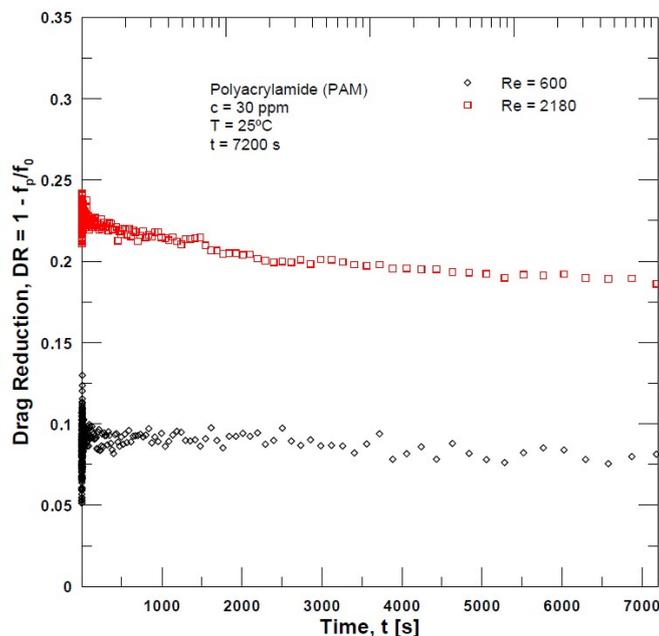

Figure 6. Polymer degradation, concentration of 30 ppm, t = 7200 s.

The polymer degradation in the transition region occurs, but much slower than in the fully turbulent region, as shown in Fig. 6. A solution with 30 ppm of PAM (in deionized water) is tested with two Reynolds, one turbulent (*Re* = 2180) and another in the transition region (Re = 600), durante 7200 s. It can be seen that for the lower Re the solution almost does not degrade, that is, there is almost no increase in the friction factor with time. However, DR fall is more noticeable in the turbulent regime, going from DR = 22% at the beginning of the run to DR = 18% at the end. This is an advantage for flow with Taylor instabilities, since there is drag reduction and there is no significant polymer degradation.

4. FINAL REMARKS

This work has shown that in fact the reduction of drag is present in the flow with Taylor instabilities (transition region), since many authors attribute this phenomenon to the interaction between the turbulent vortices and the macromolecules of polymers. It is clear and evident that drag reduction is also significant in this region (exceeding 22% for 100 and 400 ppm solutions, with Re = 920). Another interesting fact is the reduced rate of degradation of the polymer in the transition region, since the breakdown of the polymer molecules is also associated with this interaction.

5. REFERENCES.

Andereck, C.D., Liu, S.S. and Swinney, H.L., 1986. *Flow regimes in a circular Couette System with independently rotating cylinders*. J. Fluid Mech.; vol. 164, pp. 155-183.

Andrade, R.M. and Soares, E.J., 2013. *Drag reduction in seawater by polymer addition into a rotating cylindrical double gap device: effect of reynolds number, polymer concentration, and sea salt concentration*. 22nd International Congress of Mechanical Engineering (COBEM 2013). Ribeirão Preto, SP, Brazil.

Arias, B.M. and Peixinho, J., 2017. *Torque in Taylor–Couette flow of viscoelastic polymer solutions*. Journal of Non-Newtonian Fluid Mechanics; 247, pp. 221–228.

Choi, H.J., Kim, C.A., Sohn, J. and Jhon, M.S., 2000. *An exponential decay function for polymer degradation in turbulent drag reduction*. Polym. Degrad. Stabil. 69, 341–346.

Crumeyrolle, O., Mutabazi, I. and Grisel, M., 2002. *Experimental study of inertioelastic Couette–Taylor instability modes in dilute and semidilute polymer solutions*. Physics of Fluids, vol. 14, nº 5, pp. 1681-1688.

Fabula, A.G., 1971. *Fire-fighting benefits of polymeric friction reduction*. Trans ASME J Basic Engng, pp. 93–453, 1971.

Ginn, R.F. and Denn, M.M., 1969. *Rotational stability in viscoelastic liquids: Theory*. AIChE J. 15, 450.

Golda, J., 1986. *Hydraulic transport of coal in pipes with drag reducing additives*. Chem Engng Commun, vol. 45, pp. 53-67.

Gyr, A. and Tsinober, T., 1995. *On the rheological nature of drag reduction phenomena*. Journal of Non-Newtonian Fluid Mechanics, vol. 73, pp. 153–162.

Kameneva, M.V., Wu, Z.J., Uraysh, A., Repko, B., Litwak, K.N., Billiar, T.R., Fink, M.P. and Simmons, R.L., 2003. *Blood soluble drag-reducing polymers prevent lethality 85 from hemorrhagic shock in acute animal experiments*. Biorheology, vol. 41, no. 1, pp. 53–64.

Larson, R. G. 2003. *Analysis of polymer drag reduction on a flat plate*. Journal of Non-Newtonian Fluid Mechanics, vol. 111, p. 229.

Lee, S.H.K., Sengupta, S. and Wei, T., 1995. *Effect of polymer additives on Gortler vortices in Taylor-Couette flow*. Journal of Fluid Mechanics, vol. 282, pp. 115–129.

Mostardi, R.A., Thomas, L.C., Greene, H.L., VanEssen, F. and Nokes, R.F., 1978. *Suppression of atherosclerosis in rabbits using drag reducing polymers*. Biorheology, vol. 15, nº. 1, pp. 1–14.

Pereira, A.S. and Soares, E.J., 2012. *Polymer degradation of dilute solutions in turbulent drag reducing flows in a cylindrical double gap rheometer device*. Journal of Non-Newtonian Fluid Mechanics 179–180 (2012) 9–22.

Pereira, A.S., Andrade, R.M. and Soares, E.J., 2013. *Drag reduction induced by flexible and rigid molecules in a turbulent flow into a rotating cylindrical double gap device: Comparison between Poly(ethylene oxide), Polyacrylamide, and Xanthan Gum*. Journal of Non-Newtonian Fluid Mechanics, v. 202, p. 72-87.

Nakken, T., Tande, M. and Elgsaeter, A., 2001. *Measurements of polymer induced drag reduction and polymer scission in taylor flow using standard double-gap sample holders with axial symmetry*, J. Non-Newton. Fluid Mech. 97 pp. 1–12.

Sellin, R.H.J., Hoyt, J.W., Poliert, J. and Scrivener, O., 1982. *The effect of drag reducing additives on fluid flows and there industrial applications part ii: present applications and futures proposals*. J. Hydraul. Res. 20, pp. 235–292.

Toms, B.A., 1948. *Some observations on the flow of linear polymer solutions through straight tubes at large reynolds numbers, in: Proceedings of the International*. Congress of Rheology, Holland, North-Holland, Amsterdam, Section II, pp. 135–141.

Unthank, J.L.S.G., Lalka, S.G., Nixon, J.C. and Sawchuk, A.P.,1992. *Improvement of flow through arterial stenoses by drag reducing agents*. Journal of Surgical Research, vol. 53, nº. 6, pp. 625–630.

Vanapalli, S.A., Islam, T.M. and Solomon, J.M., 2005. *Scission-induced bounds on maximum polymer drag reduction in turbulent flow*, Phys. Fluids 17.

6. RESPONSIBILITY NOTICE

The authors are the only responsible for the printed material included in this paper.